

## A study of Asian dust plumes using satellite, surface, and aircraft measurements during the INTEX-B field experiment

Timothy Logan,<sup>1</sup> Baike Xi,<sup>1</sup> Xiquan Dong,<sup>1</sup> Rebecca Obrecht,<sup>1</sup> Zhanqing Li,<sup>2</sup> and Maureen Cribb<sup>2</sup>

Received 2 March 2010; revised 3 June 2010; accepted 6 July 2010; published 20 October 2010.

[1] Asian dust events occur frequently during the boreal spring season. Their optical properties have been analyzed by using a combination of source region (ground-based and satellite) and remote Pacific Ocean (aircraft) measurements during the Intercontinental Chemical Transport Experiment-Phase B (INTEX-B) field campaign which lasted from 7 April to 15 May 2006. A strong dust event originating from the Gobi Desert and passing over the Xianghe surface site on 17 April 2006 has been extensively analyzed. The surface averaged aerosol optical depth (AOD) values increased from 0.17 (clear sky) to 4.0 (strong dust), and the Angström exponent ( $\alpha$ ) dropped from 1.26 (clear sky) to below 0.1. Its total downwelling SW flux over the Xianghe site (thousands of kilometers away from the dust source region) is only 46% of the clear-sky value with almost no direct transmission and nearly double the diffuse SW clear-sky value. This event was also captured 6 days later by satellite observations as well as the UND/NASA DC-8 aircraft over the eastern Pacific Ocean. The DC-8 measurements in the remote Pacific region further classified the plumes into dust dominant, pollution dominant, and a mixture of dust and pollution events. HYSPLIT backward trajectories not only verified the origins of each case we selected but also showed (1) two possible origins for the dust: the Gobi and Taklimakan deserts; and (2) pollution: urban areas in eastern China, Japan, and other industrialized cities east of the two deserts. Based on the averaged satellite retrieved AOD data ( $0.5^\circ \times 0.5^\circ$  grid box), declining AOD values with respect to longitude demonstrated the evolution of the transpacific transport pathway of Asian dust and pollution over the period of the field campaign.

**Citation:** Logan, T., B. Xi, X. Dong, R. Obrecht, Z. Li, and M. Cribb (2010), A study of Asian dust plumes using satellite, surface, and aircraft measurements during the INTEX-B field experiment, *J. Geophys. Res.*, *115*, D00K25, doi:10.1029/2010JD014134.

### 1. Introduction

[2] Dust is a significant type of particulate that contributes to the aerosol effect, being one of the leading uncertainties in radiative forcing [Intergovernmental Panel on Climate Change, 2001, 2007]. Aerosols can have an impact on global/regional climate through its so-called “direct” and “indirect” radiative effects by changing the optical properties of the Earth’s atmosphere specifically through the scattering and absorption of both solar and thermal infrared radiation [Tanré *et al.*, 2001]. This can have a further effect of warming the layer in which the dust resides while cooling the surface [Li *et al.*, 2007a]. Dust can also influence the aerosol indirect effect by altering the size distribution of

cloud water droplets which can interfere with the hydrologic cycle.

[3] Strong episodic dust events in Asia frequently occur in the spring months between March and May [Li *et al.*, 2007a; Sun *et al.*, 2001; Dibb *et al.*, 1997, 2003; Tsunematsu *et al.*, 2005]. These events routinely originate from the Gobi Desert between Mongolia and north-central China and the Taklimakan Desert in western China. Under specific meteorological conditions (e.g., wind speeds greater than 5 m/s associated with a low-pressure system and a dry spring season), airborne mineral dust and soil can be lofted into the free atmosphere and is capable of traveling from Asia to North America via the Pacific Ocean [Tsunematsu *et al.*, 2005; Murayama *et al.*, 2001; Husar *et al.*, 2001]. As the dust plumes move eastward with prevailing winds, they can also pass over the various regions of central and eastern Asia and draw up large concentrations of dust and aerosols native to those regions into the free troposphere. How the properties of Asian dust both evolve and impact locations distant from their origin is still in question. Studying the transcontinental and transpacific transport of both dust and

<sup>1</sup>Department of Atmospheric Sciences, University of North Dakota, Grand Forks, North Dakota, USA.

<sup>2</sup>Department of Atmospheric and Oceanic Science, University of Maryland, College Park, Maryland, USA.

aerosols plays a vital role in the understanding of regional and global climate change.

[4] Over the past few decades, several field campaigns have been carried out over the western Pacific region such as the Pacific Exploratory Mission (PEM-West A and B) [Bachmeier *et al.*, 1996] and The Aerosol Characterization Experiment-Asia (ACE-Asia) along with the Transport and Chemical Evolution-Pacific (TRACE-P) in 2001 [Huebert *et al.*, 2003; Jacob *et al.*, 2003] to study the impact of dust transport on downwind regions. To further improve our understanding of sources and sinks of environmentally important gases and aerosols through the constraints of atmospheric observations, NASA led a field experiment called the Intercontinental Chemical Transport Experiment-Phase B (INTEX-B) during the spring of 2006 over the eastern Pacific Ocean (H. B. Singh *et al.*, The Intercontinental Chemical Transport Experiment-Phase B (INTEX-B): An update, 2006, [http://avdc.gsfc.nasa.gov/Documentation/Validation\\_Plan/PDF/INTEXB\\_WhitePaper.pdf](http://avdc.gsfc.nasa.gov/Documentation/Validation_Plan/PDF/INTEXB_WhitePaper.pdf)). (INTEX-B, the second phase of the main field experiment called INTEX-North America, was a two-part field experiment with the first half of INTEX-B conducted over Mexico, but for this paper, INTEX-B here only refers to the second half of the campaign over the eastern Pacific Ocean.) The major goals of INTEX-B were to quantify the transpacific transport and evolution of Asian dust and assess its implications for regional climate.

[5] This study focused on analyzing the optical properties of the dust plumes observed over both the Xianghe surface station and the remote Pacific, where the DC-8 aircraft had intensive measurements of any evidence of dust plumes that may be observed during the middle of the 2006 spring season. We also attempt to use Terra/Aqua measurements to outline the transpacific transport process during the same time period. Based on available data, we want to examine three scientific issues of Asian dust: (1) aerosol properties along with surface and top-of-atmosphere (TOA) radiation budgets, (2) aerosol properties as functions of both their points of origin and destination, and (3) the major transport pathway based on the satellite (Terra/Aqua) measured AOD. This paper reports the optical properties of Asian dust, as well as its strength and evolution from its source regions (e.g., Gobi and Taklimakan deserts) to the remote Pacific Ocean during INTEX-B. The data sets used in this study include surface, satellite (Terra/Aqua), and aircraft (University of North Dakota (UND)/NASA DC-8) observations, as well as NOAA HYSPLIT model trajectories.

## 2. Data and Methodology

[6] Several data sets have been collected and used to analyze the Asian dust in this study. Surface observed/retrieved AOD, solar irradiance, and Angström exponent ( $\alpha$ ) were collected from the East Asian Study of Tropospheric Aerosols: an International Regional Experiment (EAST-AIRE) for China [Li *et al.*, 2007b]. The satellite AOD and TOA albedo were derived from the Moderate Resolution Imaging Spectroradiometer (MODIS) and Clouds and the Earth's Radiant Energy System (CERES) observations, respectively, on Terra and Aqua satellites. The UND/NASA DC-8 aircraft participated in the INTEX-B field mission, and for this study, the NASA Langley Airborne Differential

Absorption Lidar (DIAL) and TSI 3563 integrating nephelometer data were used. The surface, aircraft, and satellite data were collected during the period of April–May 2006 for this study and are discussed in sections 2.1–2.3.

### 2.1. Surface

[7] Radiation and aerosol data in China were collected at the Xianghe (39.753°N, 116.961°E) Observatory of the Institute of Atmospheric Physics, Chinese Academy of Sciences. The observatory is located between two megacities with Beijing 70 km to the northwest and Tianjin 70 km to the southeast. This site has been taking continuous measurements of various surface radiation and aerosol quantities since September 2004. The total, direct, and diffuse downwelling shortwave (SW) radiation were measured at a 1 min temporal resolution with the Kipp and Zonnen's CM21 and CM11 radiometers, a normal incidence pyrheliometer (NIP), and a black and white pyranometer, respectively, with an uncertainty of  $\sim 5 \text{ W m}^{-2}$  [Li *et al.*, 2007a].

[8] Aerosol optical depth (AOD) was derived from the Cimel-318 Sun photometer measurements [Holben *et al.*, 1998]. The Sun photometer is a multichannel, automatic Sun-and-sky scanning radiometer with a spectral range between 340 and 1020 nm, with a total uncertainty under cloud-free conditions of  $\leq \pm 0.01$  for  $\lambda > 440 \text{ nm}$  and  $\leq \pm 0.02$  for shorter wavelengths. The AOD values were retrieved at three discrete wavelengths (440, 500, and 700 nm) and were taken 30 s apart to create the triplet observation per wavelength used in the cloud-screening process. The triplet observations were made at 15 min intervals to discriminate clouds in the variation of the triplet since the temporal variation of clouds is typically greater than that of aerosols. If any clouds were missed by the triplet observations, these outliers were removed by inspecting the AOD data for possible cloud contamination. Therefore, the AOD values used in this study exclude most cloud-contaminated data. The Angström Exponent (i.e., the slope of the spectral optical depth)  $\alpha$ , was calculated by the linear square fit slope of the spectral Sun photometer measurements as a function of wavelength on a logarithmic scale. For this study, only level 2.0 data (cloud-screened and quality-assured) were used.

[9] The total sky imager (TSI-440) takes snapshots of the sky on a continuous 1 min basis each day from sunrise to sunset. Due to the high frequency of images captured, a movie of sky conditions was generated for each day [Li *et al.*, 2007a]. Images from the TSI-440 were used to help distinguish between cloudy and dusty conditions at Xianghe. Though dust storms are generally associated with strong synoptic systems that generate clouds, the images from the TSI-440 show a difference between sky-obscuring aerosol haze and cloudiness as atmospheric aerosols tend to be less variable than clouds (i.e., on average, a haze layer can linger for a longer time period than clouds).

### 2.2. Satellite

[10] The satellite data sets used in this study were the Terra Edition2B and Aqua Edition1B CERES Single Scanner Footprint (SSF) products and include the "Rev1" calibration adjustment to the CERES shortwave (SW) record to account for optics contamination during the first few years on orbit [Matthews *et al.*, 2005]. The CERES instru-

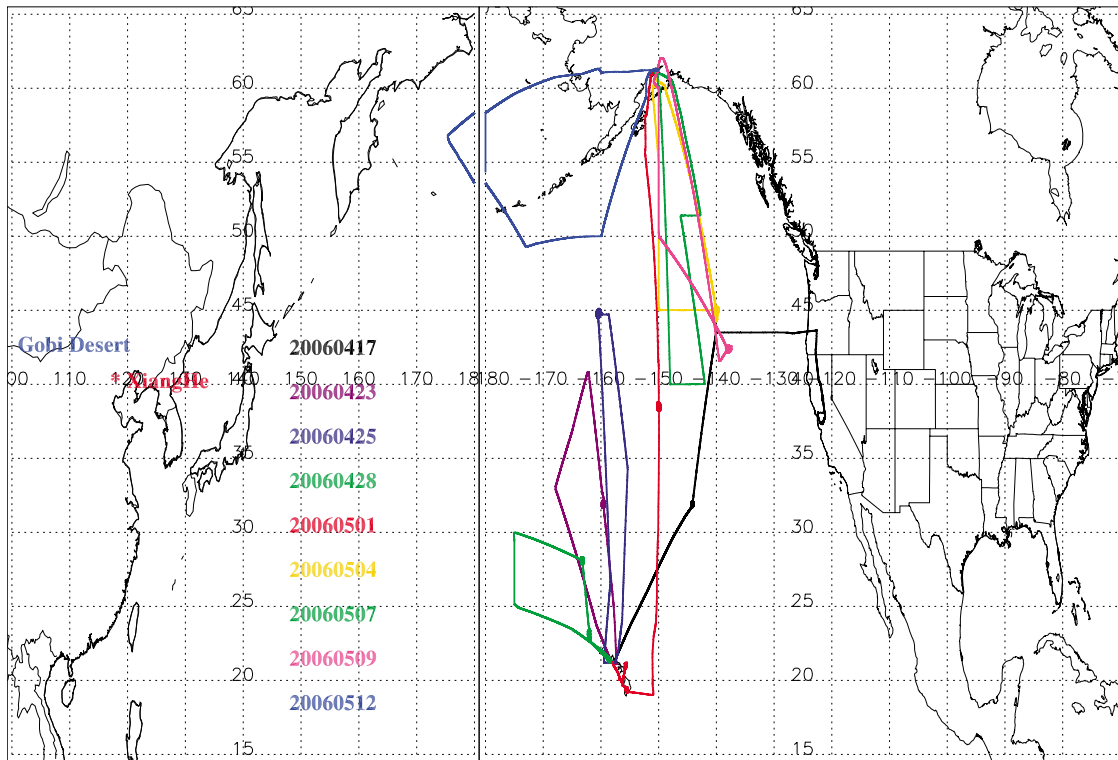


**Figure 1.** A map showing nine UND/NASA DC-8 flight tracks during INTEX-B over the remote Pacific Ocean and AERONET surface site (Xianghe, near Beijing). The solid lines are the flights used this study.

ments on the Terra and Aqua satellites measure radiances that are converted to broadband fluxes using Angular Distribution Models (ADMs) sampled and optimized for each satellite orbit. Estimated uncertainties in the solar-reflected ( $SW_{\text{toa}}^{\uparrow}$ ) single field-of-view instantaneous radiative fluxes at TOA are  $13 \text{ W m}^{-2}$  [Chambers *et al.*, 2002; Loeb *et al.*, 2003]. The SSF combines the CERES broadband flux measurements at a 20 km resolution with coincident, subsampled 1 km MODIS cloud and aerosol retrievals [Wielicki *et al.*, 1996; Ignatov *et al.*, 2005]. These data sets include the MODIS-retrieved visible (550 nm) AOD (MOD04 on Terra; MYD04 on Aqua) and CERES-derived TOA albedo over the Asian continent. The MOD04 product uses sophisticated cloud screening and aerosol retrieval algorithms developed by the MODIS cloud and aerosol groups with uncertainties of  $0.03 \pm 0.05 \text{ AOD}$  over ocean and  $0.05 \pm 0.15 \text{ AOD}$  over land [Tanré *et al.*, 1997; Ackerman *et al.*, 1998; Martins *et al.*, 2002; Remer *et al.*, 2005].

### 2.3. DC-8 Aircraft

[11] The UND/NASA DC-8 aircraft platform remotely measured the in situ aerosol properties during 10 flights (Figure 1) with a total of 85 h over the central Pacific Ocean between Hawaii and Alaska. For this study, the DIAL and nephelometer measurements were used to determine the location of dust in the atmosphere. The types of measurements used in this study include: (1) pressure altitude, longitude, and latitude (i.e., along the flight track) and (2) optical properties – aerosol scattering ratios at 588 and 1064 nm from the Differential Absorption Lidar (DIAL), aerosol scattering coefficients at 450, 550, and 700 nm from

the nephelometer, and (3) Angström exponent and spectral curvature values derived from nephelometer measurements.

[12] The DIAL measurement system, developed by the NASA Langley Research Center, measured aerosol backscattering in both visible ( $\lambda = 588 \text{ nm}$ ) and near infrared (IR,  $\lambda = 1064 \text{ nm}$ ) wavelengths [Browell *et al.*, 1998]. The vertical resolution of the DIAL measurement system was 30 m, a horizontal resolution of 2.3 km and a 10 s temporal resolution along the DC-8 flight track. The equation to calculate the aerosol scattering ratio,  $R_{\lambda}(z)$  at a given wavelength ( $\lambda$ ) is given by

$$R_{\lambda}(z) = \frac{\beta_1(z) + \beta_2(z)}{\beta_2(z)}, \quad (1)$$

where  $\beta_1(z)$  and  $\beta_2(z)$  are the backscattering coefficients ( $\sim r^6/\lambda^4$ ) by aerosols and air molecules at altitude  $z$ , respectively. Typical scattering ratios are close to 1 for regions free of aerosol, and greater than 1 for the dust plumes. Note that the cloud particles usually have a very large scattering ratio at both wavelengths because the backscattering coefficient is proportional to sixth power of particle size ( $\sim r^6/\lambda^4$ ) [Dong and Mace, 2003].

[13] For the TSI Model 3563 nephelometer onboard the DC-8 aircraft, aerosol integrated light scattering coefficients at three wavelengths in the visible spectrum (450, 550, and 700 nm) were measured. For fine mode aerosols, the aerosol scattering coefficients inversely increase with wavelengths from 450 to 700 nm, but for coarse mode aerosols the aerosol scattering coefficients are nearly independent of wavelength. Therefore, for fine mode aerosols, the slope of

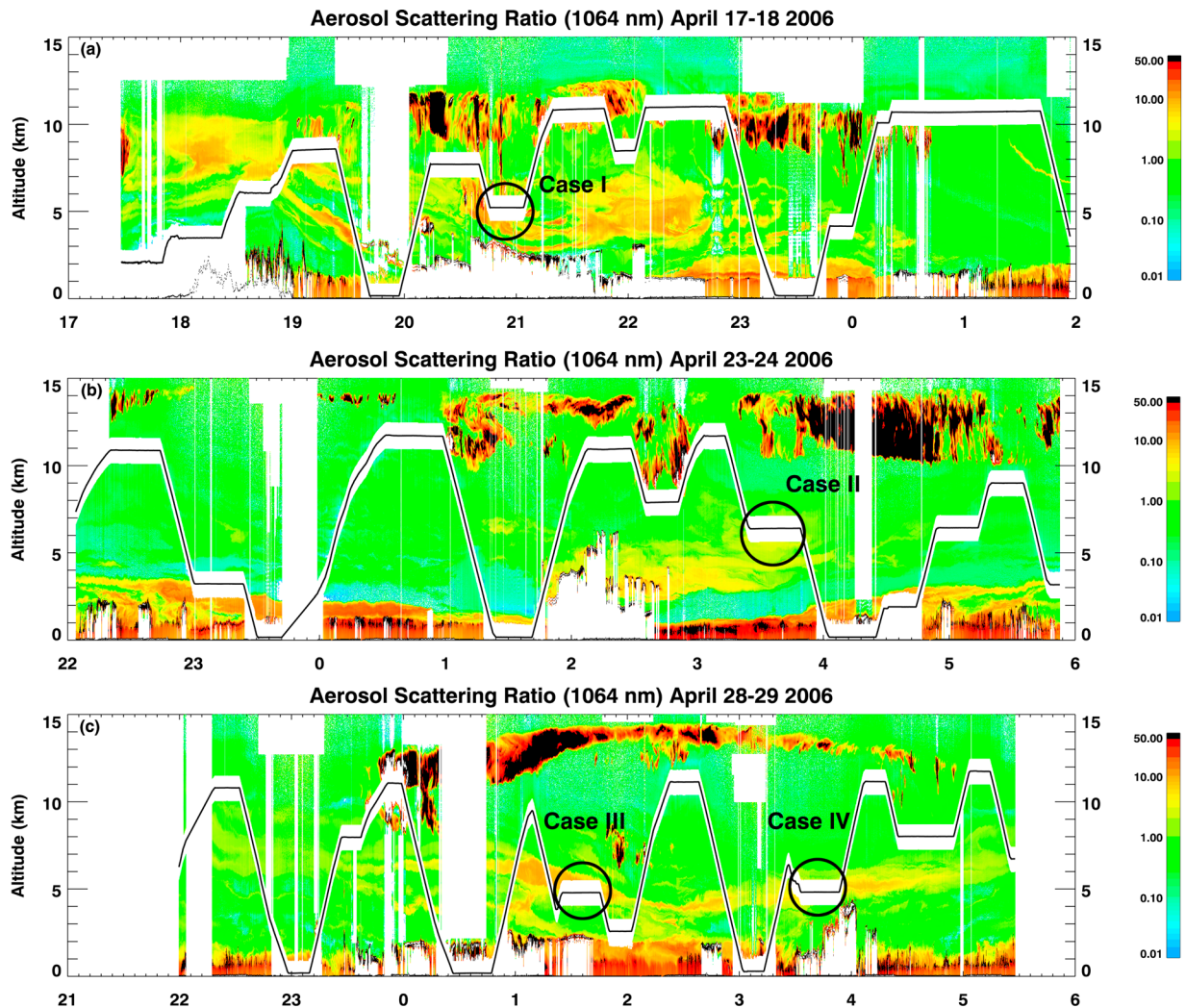


**Figure 2.** Aerosol scattering ratios observed by Differential Absorption Lidar (DIAL) on DC-8 aircraft during the INTEX-B field campaign over the remote Pacific Ocean. The four selected dust events used in this study: (a) Case I, (b) Case II, and (c) Case III and IV.

this relationship can be given by the Angström exponent ( $\alpha$ ). The equation for calculating  $\alpha$  is given by

$$\alpha = -[\log(\tau_{\lambda_1}/\tau_{\lambda_2})/\log(\lambda_1/\lambda_2)], \quad (2)$$

where  $\tau_{\lambda_1}$  and  $\tau_{\lambda_2}$  are the optical depths at two given wavelengths  $\lambda_1$  and  $\lambda_2$ . The optical depth is proportional to the aerosol scattering ratio  $\beta_\lambda$ , therefore, the ratio of  $\tau_{\lambda_1}$  and  $\tau_{\lambda_2}$  is proportional to the ratio of  $\beta_{\lambda_1}$  and  $\beta_{\lambda_2}$ . *Gobbi et al.* [2007] pointed out that  $\alpha$  is a good indicator of aerosol size in the solar spectrum:  $\alpha > 1$  represents fine mode, submicron aerosols;  $0 < \alpha < 1$  represents a mixture of coarse and fine modes;  $\alpha \sim 0$  represents existing coarse, supermicron particles.

[14] Correction factors designed by *Anderson and Ogren* [1998] were applied to the nephelometer data prior to use in this study. First, the nephelometer measurements were corrected by calibrating the instrument with gas particles since they undergo Rayleigh scattering and do not show the near-forward-scattering biases as do particles close to or greater than  $1 \mu\text{m}$  [*Anderson and Ogren*, 1998]. Second, the

nephelometer measurements were corrected to  $0^\circ$ – $180^\circ$  from its original detection angles of  $7^\circ$ – $170^\circ$ . The temporal resolution of sampling averaged roughly 10 s in order to limit instrument noise. The scattering coefficients derived from nephelometer measurements are used to distinguish the coarse mode (dust) and fine (pollution) aerosols within Asian dust plumes.

#### 2.4. Dust Plume Selection Criteria Over Source/Sink Regions and During Transport

[15] The criteria for selecting clean, cloud-free events (hereafter called clear events) are (1) direct SW more than 80% of total SW, (2) diffuse SW less than 20% of total SW, (3)  $\alpha$  greater than 1, (4) AOD values retrieved from both surface and satellite less than 0.4, and (5) high-pressure system over the Gobi Desert. Strong dust events are selected using the following criteria: (1) direct SW less than 20% of total SW, (2) diffuse SW more than 80% of total SW, (3)  $\alpha$  less than 0.3, (4) AOD values retrieved from both surface and satellite greater than 1, and (5) low-pressure system over the Gobi Desert, and very strong pressure gradient near

**Table 1.** Annual Means and Standard Deviations of  $\alpha$  Measured at Sites in the Chinese Sun Hazemeter Network (CSHNET)

Site Name	Ecosystem	$\alpha$
Fukang	desert	$0.99 \pm 0.38$
Eerduosi	desert	$0.42 \pm 0.41$
Shapotou	desert	$0.71 \pm 0.29$
Shanghai	urban	$1.08 \pm 0.24$
Lanzhou	urban	$0.90 \pm 0.23$
Beijing	urban	$1.48 \pm 0.56$

the surface site. Dust events that fall between the clear-sky and the strong dust criteria are deemed as weak events though the magnitude of their optical properties vary between the clear sky and strong dust values. All events (clear, strong, and weak) were not cloud contaminated and were identified by both TSI-440 video and MODIS visible channel images.

[16] Three conditions needed to be met before selecting the cases of Asian dust transport to the remote Pacific Ocean: (1) only the observations over remote Pacific Ocean were used, (2) DIAL aerosol scattering ratios at 1064 nm were used to determine the time periods and altitudes of the dust plumes ( $\sim 5$  km or 500 hPa) as well as discern between dust plumes and contaminants (e.g., clouds and sea salt, Figure 2), and (3) nephelometer total aerosol scattering coefficients at 450, 550, and 700 nm wavelengths were used to identify the fine and coarse model aerosols in the dust plumes. Cirrus clouds can be inferred from backscattering values of 50 and higher as well as their resident altitude of greater than 7 km. Coarse mode sea salt dominates the aerosol composition in the boundary layer over the Pacific Ocean and can bias dust plume results more toward being largely coarse mode. Data from flight legs of less than 2 km in altitude (within the boundary layer) were eliminated in order to minimize any sea salt contaminations in this study.

[17] In order to analyze the properties of dust plumes carrying mixtures of Asian dust and pollution, *Gobbi et al.* [2007] proposed a method involving both spectral curvature ( $\delta\alpha$ ) and  $\alpha$  to track mixtures of pollution with dust. Spectral curvature is defined as the change in  $\alpha$  over a range of three wavelengths and is useful in separating fine mode aerosols ( $\delta\alpha < 0$ ) from mixtures ( $\delta\alpha \sim 0$ ) [*Gobbi et al.*, 2007]. The equation for calculating  $\delta\alpha$  using the  $\alpha$  measurements at the wavelengths of 450, 550, and 700 nm is as follows:

$$\delta\alpha = \alpha_{450-700} - \alpha_{550-700} \quad (3)$$

where  $\delta\alpha$  and  $\alpha$  were related to aerosol size distribution. The values used for deriving empirical relationships in these studies ranged from  $-1$  to  $1$ . *Gobbi et al.* [2007] demonstrated that  $\delta\alpha$  can be very close to zero under the conditions of low concentration of fine aerosols. By using the relationship between  $\delta\alpha$  and  $\alpha$ , they were able to discern situations where fine mode aerosols were dominant in a modeled dust plume from a mixture of both fine and coarse mode aerosols. They further suggested that any appreciable concentration of fine aerosol particles (usually generated from the gas to particle conversion process) could affect the overall physical properties of the Asian dust plume.

[18] Table 1 gives the annual mean Angström exponent values for desert and some representative urban regions in

Asia. Desert regions have typically  $\alpha$  values less than 1 due to the presence of coarse mode particles while urban areas that are dominated by fine mode pollution particles have  $\alpha$  values greater than 1. In some urban area such as Lanzhou which locates downwind of Gobi Desert, its annual mean  $\alpha$  are very close to 1. This is one of the best examples for well mixed urban pollution and the dust particles. Coexistence of coarse and fine particles is evidenced at the polluted sites downwind of arid regions [*Gobbi et al.*, 2007].

### 3. Results and Discussions

[19] In this study, only one event for each of the following categories of sky conditions: the clear-sky, strong dust, strong pollution, and mixed pollution with dust categories is presented. Backward trajectories are used to track the dust events to the eastern Pacific where these events were observed by the DC-8 DIAL and nephelometer measurements in addition to satellite retrievals. Backward trajectories are also used to obtain information on the possible origins of the dust plumes as they travel from the Asian mainland to the remote Pacific Ocean.

#### 3.1. Clear Sky (Clean, No Dust, Cloud-Free)

[20] To determine the baseline and provide the background values for studying Asian dust at Xianghe, China, a clear-sky event on 10 May 2006 is analyzed first with surface and satellite data. As shown in Figure 3a, the maximum total, direct, and diffuse downwelling SW fluxes are  $1003 \text{ W m}^{-2}$ ,  $849 \text{ W m}^{-2}$ , and  $160 \text{ W m}^{-2}$ , respectively. These values represent the typical meteorological conditions of a cloud-free day, when aerosol loading is low and SW scattering/absorbing is mainly due to atmospheric molecules. The surface AOD and  $\alpha$  values are nearly constant throughout the whole day with the averages of 0.17 (at  $\lambda = 500$  nm) and 1.26, respectively. Comparing the Xianghe  $\alpha$  values with the annual mean of Beijing (the nearest city) indicates that fine mode particles may have dominated in this event (Figure 3b).

[21] As illustrated in Figures 4a and 4b, the AOD values ( $\sim 0.16$ – $0.2$ ) retrieved from MODIS over the surface site are very close to the surface retrieved AOD, and the TOA albedo is also low ( $\sim 0.2$ ). The MODIS visible channel image (Figure 4c) further proves that this is a clear-sky event with little aerosol loading right over the surface site, but has some aerosol loading about 200 km south of the surface site (Figure 4c) and clouds in the southeast region. In Figure 4d, the NCEP daily averaged sea level pressure (SLP) showed a high-pressure system extending from the northwest over the Gobi Desert to Xianghe during this event. The subsidence associated with the high-pressure system as well as a weak pressure gradient kept wind speeds low at the surface and suppressed any dust or aerosols from lifting high into the atmosphere. Therefore, the integrated observations provide accurate dust-free background information for us to investigate the dust events.

#### 3.2. Dust Events

[22] As discussed in the beginning of this section, both surface and satellite observations/retrievals were used to identify and classify dust events into two main categories: (1) weak and (2) strong, as determined by their optical, physical, and strength of the synoptic system in their source

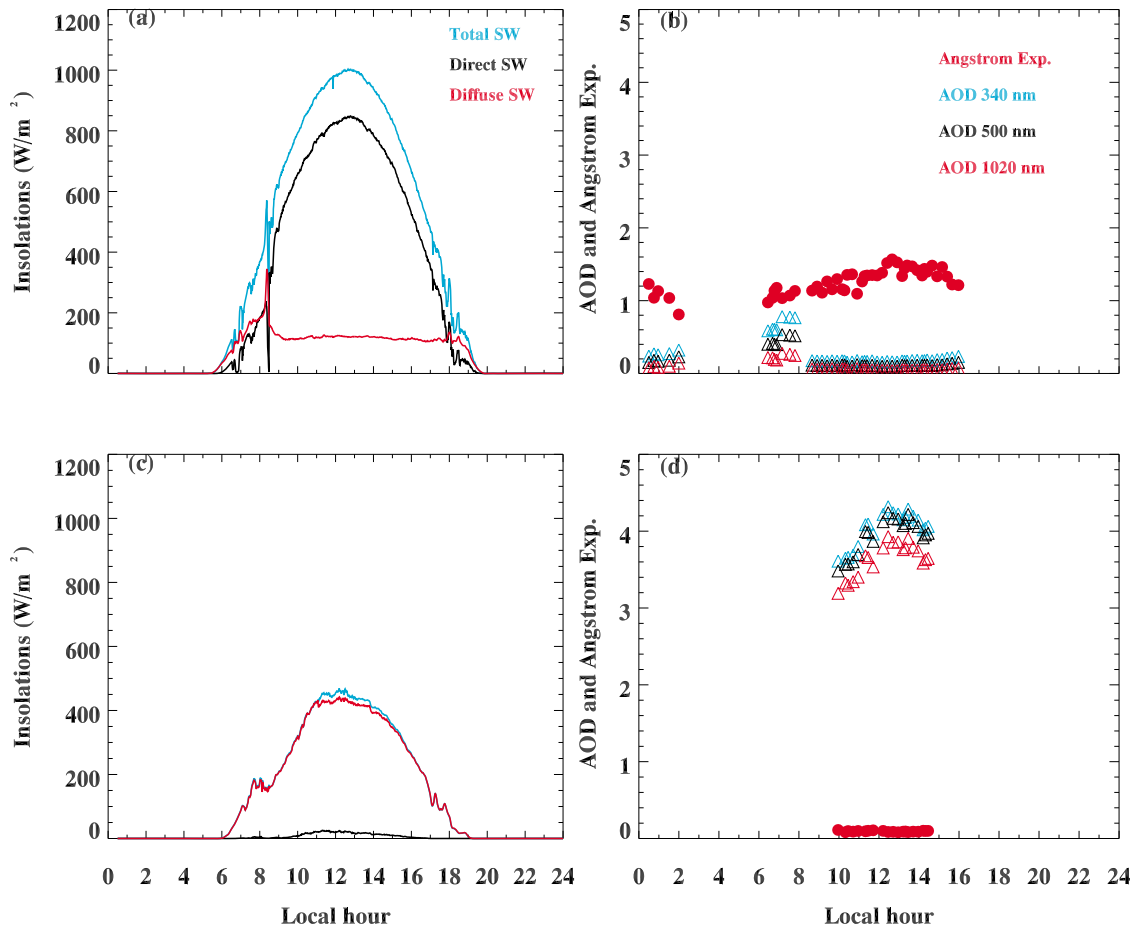


**Figure 3.** The total, direct, and diffuse downwelling shortwave (SW) fluxes measured at the Xianghe site. Aerosol optical depth (AOD) was derived from the Cimel-318 Sun photometer measurements. (a, b) Clear-sky event and (c, d) strong dust event.

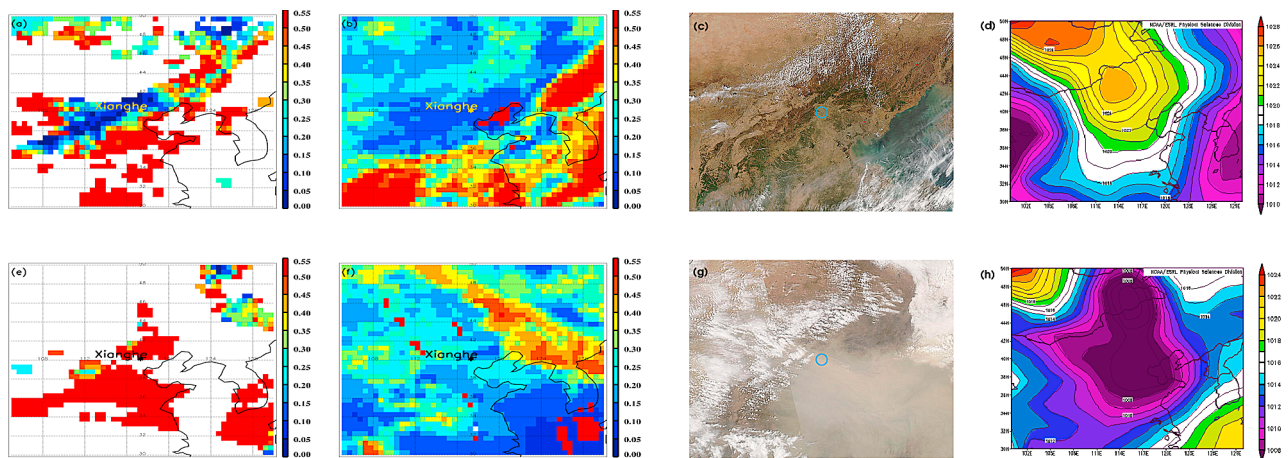


**Figure 4.** (a, e) Retrieved AOD from MODIS, (b, f) observed TOA albedo from CERES, (c, g) MODIS visible image, and (d, h) pressure pattern, for clear-sky event on 10 May 2006 (Figures 4a–4d) and for strong dust event on 17 April 2006 (Figures 4e–4h). Note that the red color in Figures 4a and 4e represents the AOD values  $\geq 0.55$ .

**Table 2a.** Summary of the Physical and Optical Properties of the Asian Dust Event Over the Source Region (Xianghe, China) During the INTEX-B<sup>a</sup>

Measurement	Clear Sky	Strong Dust	Weak Dust
<i>Surface Observations</i>			
Total SW	1000 W/m <sup>2</sup>	500 W/m <sup>2</sup>	900 W/m <sup>2</sup>
Direct SW	85%	10%	70%
Diffuse SW	15%	90%	30%
AOD	0.25 ± 0.14(92)	2.0 ± 1.34(69)	0.92 ± 0.49(122)
Angstrom Exponent	1.27 ± 0.17(92)	0.14 ± 0.15(69)	0.36 ± 0.19(122)
Pressure	high	low	low
<i>Satellite Observations</i>			
AOD	0.29 ± 0.11 (11)	1.12 ± 0.89 (16)	0.78 ± 0.23 (12)
Albedo	16.34% ± 0.87% (11)	24.89% ± 9.21% (34)	19.23% ± 11.24% (16)
Visible	clear	strong yellow appearance	hazy

<sup>a</sup>The weak dust event is a brief comparison to the clear sky and strong dust events.

region. These dust events are then summarized in Tables 2a and 2b.

### 3.2.1. Strong Dust Event Over Xianghe

[23] An intense Asian dust storm occurred over the Xianghe site on 17 April 2006 as shown in the MODIS visible channel image (Figure 4g) and reported by local observers on the ground. The Bohai Sea is completely obscured by the dust layer, the averaged AOD and TOA albedo over the Xianghe site are 0.76 and 25%, respectively (Figures 4e and 4f). This dust event was driven by a strong low-pressure system (Figure 4h) that swept over Mongolia, the Gobi Desert, and passed over Xianghe. Consistent with the satellite observations, the TSI-440 movie at the Xianghe site showed no clouds over the site, indicating that the dust almost completely obscured the sun (i.e., no direct SW transmission).

[24] Figure 3c presents the total, direct and diffuse downwelling SW fluxes, and their corresponding maximum values at the Xianghe site on 17 April 2006. The direct SW is no more than 25 W m<sup>-2</sup> and diffuse SW accounts for 90% or greater of the total incoming solar radiation due to the large amount of scattering by the aerosol particles. The AOD and  $\alpha$  values over the Xianghe site are greater than 4.0 and less than 0.1, respectively (Figure 3d), and are consistent with the surface SW observations. This  $\alpha$  value corresponds to the value for strong dust (desert source region) given in Table 1. Since Xianghe is close to Beijing, a value greater than one is expected, however, the retrieved  $\alpha$  value is much less than one for this event, indicating that the dust loading significantly altered the optical properties over the region.

[25] The nearly diminished direct SW transmission can also be explained by radiative transfer theory ( $T \sim e^{-\tau}$ ). The impact of this strong dust event on surface SW radiation budget is significant with the significant reduction in total and direct and an increase in diffuse radiation. Compared to

the clear-sky maximum SW observations, its total and direct SW transmissions have been reduced 53% and 97%, respectively, whereas its diffuse SW transmission increased 177%. Averaged AOD increases from 0.17 (clear-sky average) to 4.0 (strong dust), and  $\alpha$  drops from 1.26 (clear sky) to below 0.1. Although these results are based on the point of observations over the Xianghe site, they are consistent with dust laden air from desert regions (Table 1). *Xia et al.* [2007] studied the effects of aerosols on the surface radiation budget in northeastern China and found that the direct SW flux could be reduced by up to  $-522 \text{ W m}^{-2}$  per unit of AOD with 66% of the reduction being offset by an increase in diffuse SW flux.

[26] Although the MODIS-retrieved AOD values over the surface site are not as large as the surface retrievals, the high AOD values over areas south of the Xianghe site correspond nicely with this dust event. The large AOD difference between surface and MODIS retrievals in this case indicates the MODIS aerosol retrieval algorithm for strong dust events over land may need to be improved. The averaged TOA albedo is 25% over the surface site, which is an increase of 10% (absolute) from the clear-sky value. From radiative transfer calculations and observations in this study, increasing AOD (up to 4) can slightly increase the TOA albedo, but can significantly impact downwelling SW transmission, especially for direct SW (Figure 3c).

### 3.3. Asian Dust and Aerosol Transport Pathways as Observed by Satellite and DC-8

[27] Figure 5 shows the averaged AOD values retrieved from MODIS observations on Terra and Aqua during the INTEX-B period (from 7 April 2006 to 15 May 2006). The major pathways of aerosol plumes as observed from both Terra and Aqua are quite consistent, but the absolute values are slightly different over the land regions. As illustrated in Figure 5a and 5b, there are two dust plumes: the pollution

**Table 2b.** Summary of the Physical and Optical Properties of the Asian Dust Event Over the Remote Pacific Ocean During the INTEX-B Measured by DC-8

Case	Mean Angstrom Exponent	Mean Spectral Curvature	Remarks
Case I	0.46 ± 0.63	-0.49 ± 1.61	strong dust plume
Case II	1.53 ± 0.23	-0.31 ± 0.63	strong pollution plume
Case III	0.40 ± 0.36	-0.25 ± 0.97	mixture of strong dust and pollution
Case IV	0.60 ± 0.29	-0.23 ± 0.89	mixture of strong dust and pollution

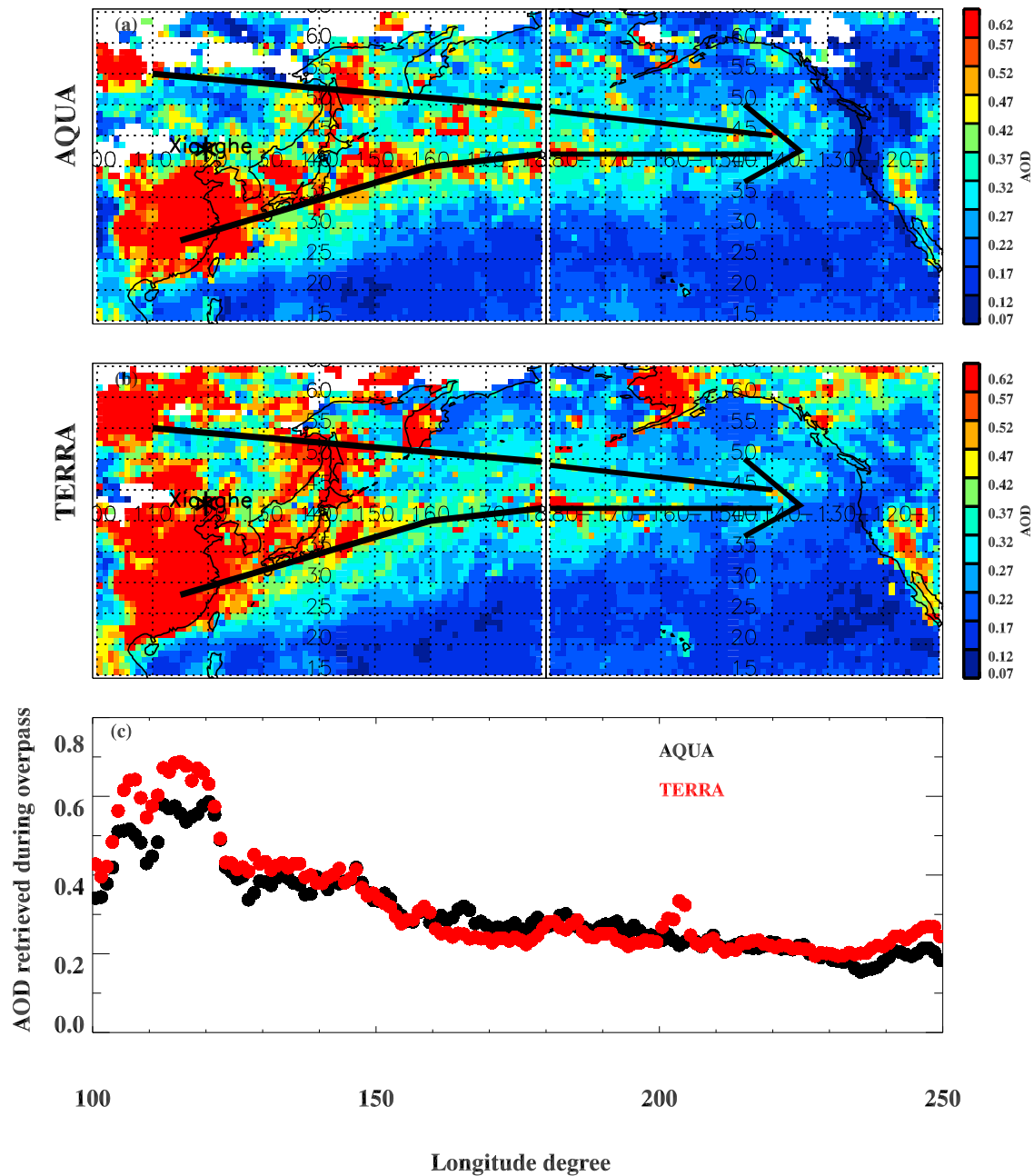


**Figure 5.** Averaged MODIS AOD values with a  $0.5^\circ \times 0.5^\circ$  grid box during the period 17 April to 15 May 2006 on (a) Aqua and (b) Terra, and (c) their transpacific transport overall zonal trend.

plume (bottom arrow) and the dust plume (top arrow) originated from two different source regions. Note that there is a large gap in both Terra and Aqua (white, no retrievals from MODIS) over Mongolia, which may represent very high AODs which cannot be retrieved by the current MODIS aerosol retrieval algorithm. Both dust plumes originated from two different regions which have two different paths that finally meet over the remote Pacific. In this study, we intend to qualitatively demonstrate the plume pathway trend using the Terra/Aqua observations, but not quantitatively address the absolute difference of their AOD retrievals, which is beyond the scope of this study. Transpacific transport during INTEX-B appears to have a steady northeasterly direction as barely any aerosols are found

below  $35^\circ\text{N}$  latitude once they reach the eastern Remote Pacific. Though there are indications of meridional flow in certain individual cases, the general flow across the Pacific for the aerosols is zonal.

[28] Plume characteristics are given by the AOD values from both the Terra and Aqua retrievals. As the aerosols are transported across the Pacific Ocean, they are prone to both wet and dry deposition as well as dispersion over time. Figure 5c shows a steady decline in aerosol optical properties over time along their transport pathway. The concentration of fine mode aerosols generally decreases in the absence of dust but when mixed with dust, heterogeneous chemical reactions can occur which may cause a slow degradation of the total aerosol layer [Leitch *et al.*, 2009].

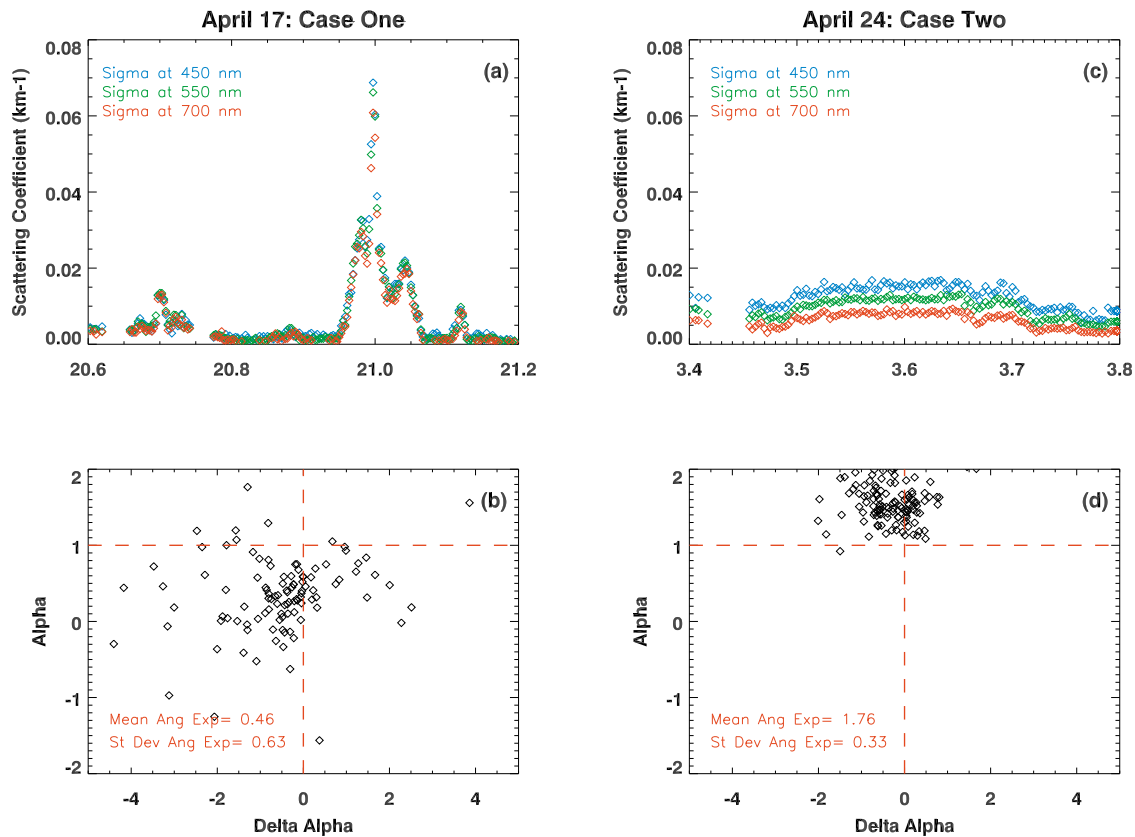


**Figure 6.** (a, b) The Case I (17 April 2006) and (c, d) Case II (24 April 2006) used in this study. The scattering coefficients at three wavelengths (450, 550, and 700 nm) (Figures 6a and 6c), and Angström exponent  $\alpha$  versus spectral curvature as observed by the TSI Model 3563 nephelometer onboard the DC-8 aircraft during the INTEX-B field campaign (Figures 6b and 6d).

For example, the AOD values peak over the east coast of China, then drop significantly over the East China Sea, and eventually level off to the values close to 0.2 as they approach the remote Pacific. The major plume transport pathway can be seen clearly by following the retrieved AOD values which suggests: plumes exiting the Asian mainland containing very high AOD values transport slightly north-east, then turn slightly eastward after passing through the middle of the Pacific until reaching close to the 145° meridian, and ultimately turn northeast toward the west coast of Canada.

[29] The time periods and altitudes of dust plumes for all flight tracks over the remote Pacific can be easily identified by using DIAL measurements of aerosol scattering ratios at 1064 nm (Figure 2). However, it is difficult to quantitatively analyze the dust plumes by using the DIAL measurements only, especially for discerning the fine and coarse mode aerosols in the dust plumes. Therefore, it is necessary to use the nephelometer data to do further study. Nephelometer data in conjunction with the technique developed by *Gobbi et al.* [2007] are utilized to verify which mode (fine or coarse) aerosols dominated in the selected four dust plumes. Scattering ratios and Angström exponent values are used as proxies for both Asian dust and pollution (Figures 6 and 7).

[30] For the 17 April 2006 dust event (Case I), the spectral data show a weak wavelength dependence of scattering coefficient values at three different wavelengths (Figure 6a)

until a peak at 2100 UTC appears where the wavelength dependence increases suddenly. Immediately after the peak, the dependence becomes negligible. Figure 6b shows that the mean (and standard deviation)  $\alpha$  is  $0.46 \pm 0.63$ , suggests that an abundance of coarse mode particles existed in the plume as given by values in Table 1. The scattering coefficients and  $\alpha$  values in Figures 6a and 6b indicate that coarse mode aerosols are dominant in the Case I.

[31] The 24 April 2006 dust event (Case II, Figure 6c) shows a strong wavelength dependence of the scattering coefficients at three wavelengths. The scattering coefficients at the shorter wavelength ( $\lambda = 450$  nm) are consistently larger than those at the higher wavelength ( $\lambda = 700$  nm) because the backward scattering coefficients decrease with increasing the wavelength with the presence of fine mode aerosols in the plume. The averaged  $\alpha$  (Figure 6d) is  $1.53 \pm 0.23$  and the  $\delta\alpha$  values lie mostly in the negative range with a mean value of  $-0.31 \pm 0.63$ , which indicates an influence of Asian pollution in this case (Table 1).

[32] The 29 April 2006 dust events (Cases III and IV, Figure 7) were observed at different time periods (Figure 2c). The  $\alpha$  values were  $0.40 \pm 0.36$  for Case III and  $0.60 \pm 0.29$  for Case IV with both being less than the Case II values. The  $\alpha$  values for Case III and IV, however, are less and greater, respectively, than those in Case I, indicating a mixture of coarse and fine mode aerosols within both dust events. For Case III, the scattering coefficients at the three wavelengths

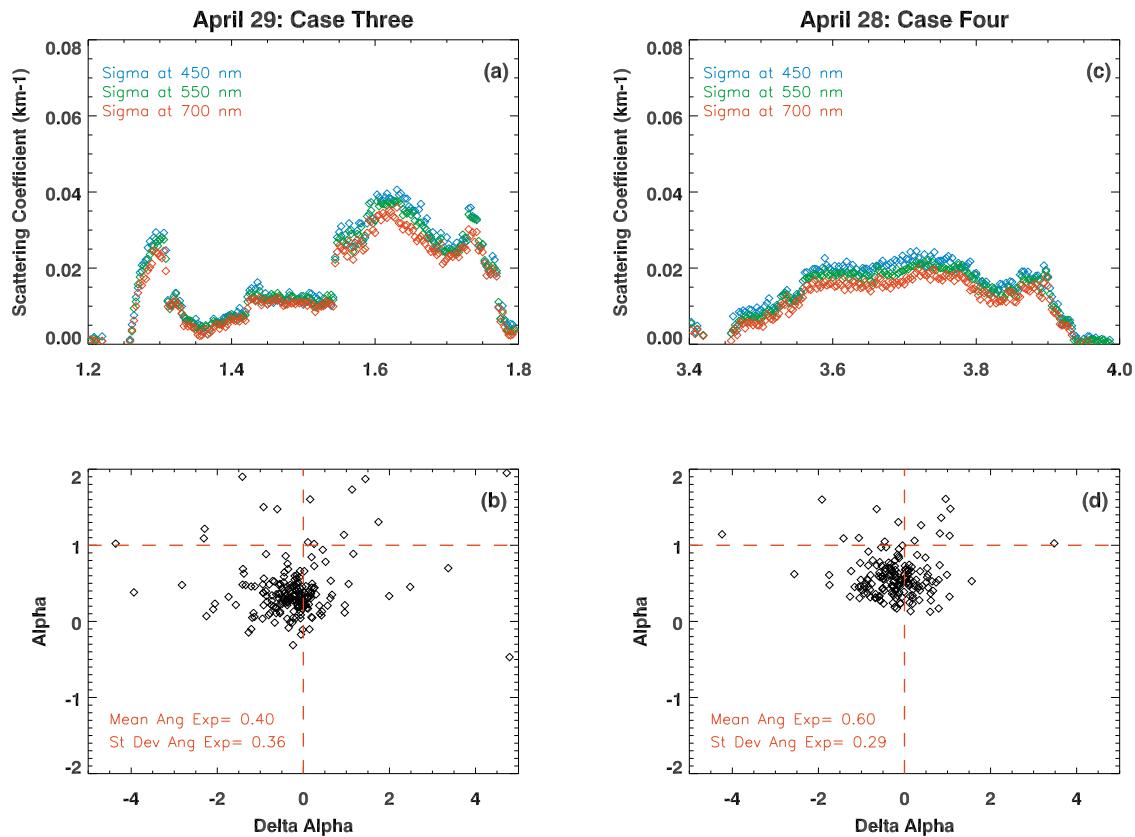


Figure 7. Same as Figure 6 for Cases III and IV.

are nearly the same (as those in Case I) during the period 1.3–1.54 UTC (Figure 7a); subsequently, sharp peaks and strong wavelength dependence occurred for the scattering coefficients after that (as those in Case II). The spectral dependences also strongly increased during the period of 1.54–1.77 UTC (not shown here). Case IV had a wavelength dependence throughout the time interval though not as strong in magnitude as Case II. Case IV had a larger  $\alpha$  mean value as compared to Case III which suggests even more fine aerosols or pollution but again, not as much as Case II.

[33] To further track these four cases back to their regions of origin, we used the NOAA backward trajectory model at three different altitudes: 3 km, 5 km, and 7 km AGL (R. R. Draxler and G. D. Rolph, HYSPLIT (Hybrid Single-Particle Lagrangian Integrated Trajectory) Model, 2003, <http://www.arl.noaa.gov/ready/hysplit4.html>). According to *Qiu and Sun* [1994], aerosol dust particles can be transported eastward from China to the Pacific Ocean in the 2 to 7 km height range, and this is the reason to choose these three altitudes in this study. It should be noted that the altitudes used in some of the HYSPLIT analyses may differ from the chosen levels as dust plume altitudes will change during transport.

[34] Figure 8 shows the back-trajectory analysis of the selected four cases (using the 5 km (blue) trajectory line as a proxy for plume altitude). Key points describing the similarities and differences from the model output include: (1) for Cases I and III, the dust plumes originated from the Gobi Desert, and (2) for Cases II and IV, the dust plumes origi-

nated from the Taklimakan desert. The transport time of dust plumes for the four cases are around 7.5, 8, 5, and 7 days, to reach the remote Pacific regions where the dust plumes were observed by the DC-8 aircraft. However, the transport time was only approximated because the measurements were not taken at the same location. From previous studies, the dust plumes normally take, on average, 7 to 10 days to move out of the Gobi Desert area to the United States. Therefore, the model outputs are 240 h in duration in order to explore all possible sources of the air masses.

[35] For Case I, the center height of dust plumes is around 5 km, ranging from 3 to 7 km (Figure 2a). From the back trajectory analysis, the blue and red lines (Figure 8a) originated from the Gobi Desert area and did not pass over the highly polluted area, whereas for Case II, the dust and pollution plume was located around 5–7 km and sampled by DC-8 at roughly 7 km (Figure 2b). The back trajectory showed that the green and blue lines originated from the Taklimakan desert and did pass through highly polluted areas. Therefore, the outputs of the back trajectory model did support the findings from DC-8 measurements in Cases I (coarse mode) and II (fine mode).

[36] For Cases III and IV, the green and blue lines originated from central China, and the data suggested a possible scenario of air masses containing dust plumes that were lifted above the boundary layer and passed through many urban areas (Figures 8c and 8d). Trajectories that come from different regions but cross paths over either the Gobi or Taklimakan Deserts are also scrutinized in order to see how

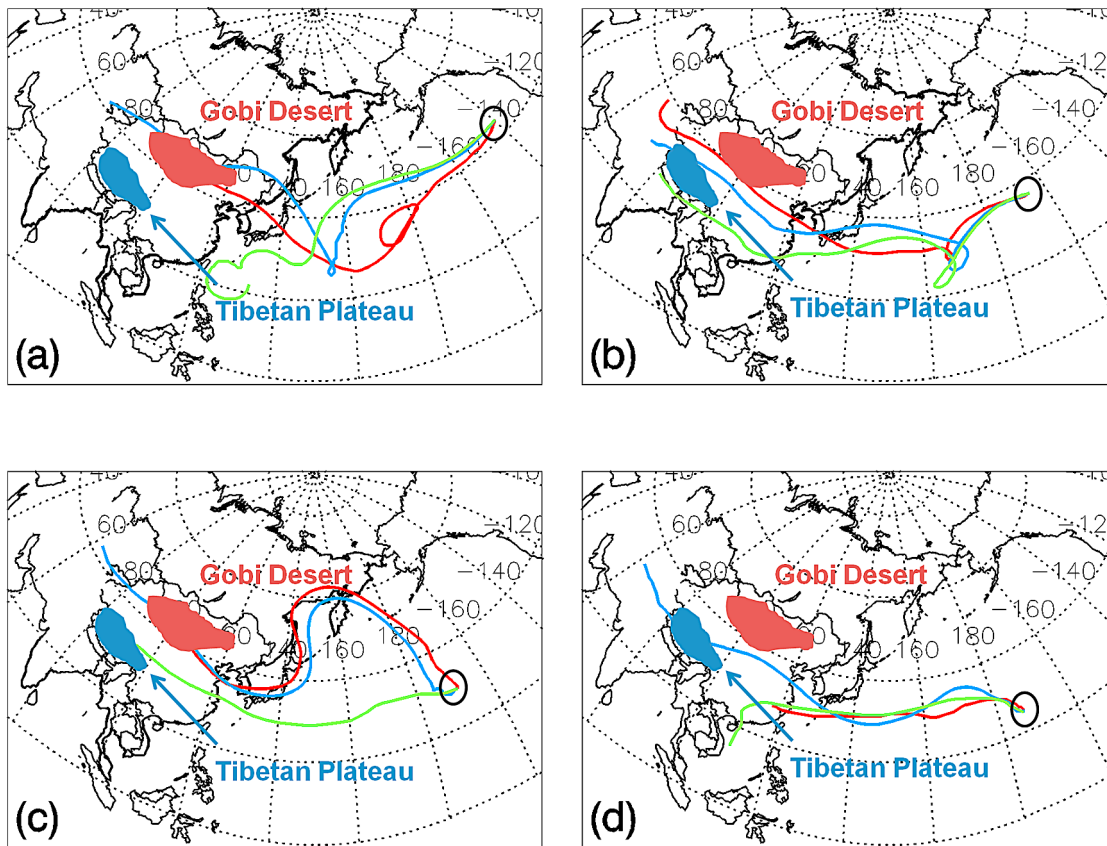


**Figure 8.** The NOAA HYSPLIT Backward Trajectories of dust plumes intercepted by DC-8 aircraft (denoted by black circles) over the remote Pacific Ocean for (a) Case I (2100 UTC 17 April 2006), (b) Case II (0300 UTC 24 April 2006), (c) Case III (0200 UTC 29 April 2006), and (d) Case IV (0400 UTC 29 April 2006). The heights of the dust plumes used in the analysis, 3000 m (red line), 5000 m (blue line), and 7000 m (green line), represent the range of heights of the dust plume intercepted by the DC-8 aircraft.

pollution and dust can come together at various points during their transpacific transport processes.

#### 4. Summary and Conclusions

[37] Tables 2a and 2b summarize the measurements and retrievals from surface, satellite, and DC-8 aircraft observations of dust events. These results were based on two clear-sky cases, six strong dust events, and five weak dust events during the April–May 2006 INTEX-B field experiment. The values in the clear-sky (clean, no dust) column provide background information and can be used as a baseline for identifying the dust events originating at East Asia, as well as for studying their strength and time evolution during the transpacific transport.

[38] Over the source region, the averaged total downwelling SW flux at surface is  $1000 \text{ W m}^{-2}$  during the clear-sky condition, including 85% of direct and 15% of diffuse transmissions. The averaged surface observed/retrieved AOD and  $\alpha$  are 0.25 and 1.27, and the averaged MODIS AOD and CERES TOA albedo are 0.29 and 16.3% under clear-sky conditions. For the strong dust events, their averaged total downwelling SW flux is only 50% of the clear-sky average, and their averaged direct and diffuse SW transmissions contribute 10% and 90% of total SW trans-

mission, respectively, which is opposite to the clear-sky results. Their averaged AOD ( $\sim 2$ ) is higher, while their averaged  $\alpha$  (0.14) is lower, than their clear-sky counterparts. The satellite retrieved AOD and TOA albedo are 1.12 and 25%, which is consistent with the surface observations. For the weak dust events, their averaged values fall between the clear-sky and strong dust results. For example, their averaged total downwelling SW flux is 90% of clear-sky mean, AOD is around 0.78–0.92,  $\alpha$  is 0.36, and TOA albedo is 19%.

[39] Over the remote Pacific Ocean the ongoing evolution of the dust plumes was tracked by examining their optical properties for the four selected cases. From the four cases, it was shown by DC-8 aircraft data (optical measurements) that the Asian dust plumes were in various states of existence suggesting an interaction between Asian dust and pollution during transport. The spectral data can also infer the plume radiative properties depending on which aerosol mode (coarse or fine) dominates within the plume. The aerosol scattering coefficients for Case I had the weakest wavelength dependence which suggested strong dust loading. From the back trajectory analysis, the blue and red lines passed over the Gobi Desert and did not pass through highly polluted areas, which strongly supports the findings from DC-8 measurements. The aerosol scattering coefficients for

Case II had the strongest wavelength dependence where the large Angström exponent ( $\alpha > 1$ ) for this case suggested that the dust plume was dominated by pollution, which was further proven by back trajectory analysis. For Cases III and IV, the magnitude of wavelength dependence fell between those found in Cases I and II (i.e., a mixture of coarse and fine mode aerosols in these two dust plumes as supported by the back trajectory analysis).

[40] These results provide invaluable information for quantifying the optical properties of Asian dust/pollution as well as their strength and evolution from their source to the remote Pacific regions. However, some overlying issues exist. For example, there are either no retrievals or lower AOD values (compared to the surface retrievals) during the strong case events over the land regions. The NASA MODIS Deep Blue aerosol retrievals, which have been improved significantly over the land regions, should be used in the future work [Hsu et al., 2004, 2006]. Though the NOAA HYSPLIT can verify the origins of aerosol and dust plumes, it is unable to account for any deposition along the transport pathway. Therefore, a more robust dust aerosol model should be used to account for both dry and wet deposition processes in future studies. As based on the results of this study, a second paper on the chemical composition of the dust plume aerosols during the INTEX-B and how they interact with one another during transport out of Asia has been done. Eventually, both of these studies will help climate and atmospheric chemistry modelers get more accurate estimations of such extreme aerosol loading at the source and along the transport pathway.

[41] **Acknowledgments.** The Xianghe observatory is operated by the Institute of the Atmospheric Physics in cooperation with the University of Maryland, and AERONET data at Trinidad Head, California, Rimrock, Idaho, and Egbert, Ontario, were provided and maintained by PIs Ellsworth G. Dutton, Brent Holben, and Norm O'Neill, respectively. The DC-8 DIAL (Edward V. Browell, PI) and nephelometer (Antony Clarke, PI) data were downloaded from the NASA LaRC INTEX-B website. The CERES SSF data were obtained from the Atmospheric Science Data Center at the NASA Langley Research Center. The HYSPLIT transport model was provided by the NOAA Air Resources Laboratory (ARL) and can be found at the READY website (<http://ready.arl.noaa.gov/HYSPLIT.php>). The University of North Dakota authors were also supported by NSF under grant ATM0649549, the NASA CERES project under grant NNL04AA11G, and the NASA NEWS project under grant NNX07AW05G, and UMD investigators were supported by the MOST (2006CB403706), NASA (NNX08AH71G) and DOE (DEFG0208ER64571) grants. Tim Logan was partially supported the North Dakota Space Grant Consortium research fellowship directed by Suzette Bieri. Additional thanks go to Jianglong Zhang, Yujun Qiu, Aaron Kennedy, Yingxi Shi, Behnjamin Zib, and Brandon Austin, who provided helpful comments and suggestions for this manuscript.

## References

- Ackerman, S., K. Strabala, P. Menzel, R. Frey, C. Moeller, and L. Gumley (1998), Discriminating clear sky from clouds with MODIS, *J. Geophys. Res.*, *103*(D24), 32,141–32,157, doi:10.1029/1998JD200032.
- Anderson, T. L., and J. A. Ogren (1998), Determining aerosol radiative properties using the TSI 3563 integrating nephelometer, *Aerosol Sci. Technol.*, *29*(1), 57–69, doi:10.1080/02786829808965551.
- Bachmeier, A. S., R. E. Newel, M. C. Shipham, Y. Zhu, D. R. Blake, and E. V. Browell (1996), PEM-West A: Meteorological overview, *J. Geophys. Res.*, *101*(D1), 1655–1677, doi:10.1029/95JD02799.
- Browell, E. V., S. Ismail, and W. B. Grant (1998), Differential absorption lidar (DIAL) measurements from air and space, *Appl. Phys. B*, *67*, 399–410, doi:10.1007/s003400050523.
- Chambers, L. H., B. Lin, and D. F. Young (2002), Examination of new CERES data for evidence of tropical Iris feedback, *J. Clim.*, *15*, 3719–3726, doi:10.1175/1520-0442(2002)015<3719:EONCDF>2.0.CO;2.
- Dibb, J. E., R. W. Talbot, B. L. Lefer, E. Scheuer, G. L. Gregory, E. V. Browell, J. D. Bradshaw, S. T. Sandholm, and H. B. Singh (1997), Distributions of beryllium 7 and lead 210, and soluble aerosol-associated ionic species over the western Pacific: PEM West B, February–March 1994, *J. Geophys. Res.*, *102*(D23), 28,287–28,302, doi:10.1029/96JD02981.
- Dibb, J. E., R. W. Talbot, E. M. Scheuer, G. Seid, M. A. Avery, and H. B. Singh (2003), Aerosol chemical composition in Asian continental outflow during the TRACE-P campaign: Comparison with PEM-West B, *J. Geophys. Res.*, *108*(D21), 8815, doi:10.1029/2002JD003111.
- Dong, X., and G. G. Mace (2003), Profiles of low-level stratus cloud microphysics deduced from ground-based measurements, *J. Atmos. Oceanic Technol.*, *20*, 42–53, doi:10.1175/1520-0426(2003)020<0042:POLLSC>2.0.CO;2.
- Gobbi, G. P., Y. J. Kaufman, I. Koren, and T. F. Eck (2007), Classification of aerosol properties derived from AERONET direct sun data, *Atmos. Chem. Phys.*, *7*, 453–458, doi:10.5194/acp-7-453-2007.
- Holben, B. N., et al. (1998), AERONET—A federated instrument network and data archive for aerosol characterization, *Remote Sens. Environ.*, *66*, 1–16, doi:10.1016/S0034-4257(98)00031-5.
- Hsu, N. C., S. C. Tsay, M. D. King, and J. R. Herman (2004), Aerosol properties over bright-reflecting source regions, *IEEE Trans. Geosci. Remote Sens.*, *42*, 557–569, doi:10.1109/TGRS.2004.824067.
- Hsu, N. C., S. C. Tsay, M. D. King, and J. R. Herman (2006), Deep Blue retrievals of Asian aerosols properties during ACE-Asia, *IEEE Trans. Geosci. Remote Sens.*, *44*, 180–183.
- Huebert, B. J., T. Bates, P. B. Russell, G. Shi, Y. J. Kim, K. Kawamura, G. Carmichael, and T. Nakajima (2003), An overview of ACE-Asia: Strategies for quantifying the relationships between Asian aerosols and their climatic impacts, *J. Geophys. Res.*, *108*(D23), 8633, doi:10.1029/2003JD003550.
- Husar, R. B., et al. (2001), Asian dust events of April 1998, *J. Geophys. Res.*, *106*(D16), 18,317–18,330, doi:10.1029/2000JD900788.
- Ignatov, A., P. Minnis, N. Loeb, B. Wielicki, W. Miller, S. Sun-Mack, D. Tanré, L. Remer, I. Laszlo, and E. Geier (2005), Two MODIS aerosol products over ocean on the Terra and Aqua CERES SSF datasets, *J. Atmos. Sci.*, *62*, 1008–1031, doi:10.1175/JAS3383.1.
- Intergovernmental Panel on Climate Change (2001), *Climate Change 2001: The Scientific Basis, Contribution of Working Group I to the Third Assessment Report of the Intergovernmental Panel on Climate Change*, edited by J. T. Houghton et al., Cambridge Univ. Press, New York.
- Intergovernmental Panel on Climate Change (2007), *Climate Change 2007: The Physical Science Basis. Contribution of Working Group I to the Fourth Assessment Report of the Intergovernmental Panel on Climate Change*, edited by S. Solomon et al., Cambridge Univ. Press, New York.
- Jacob, D. J., J. H. Crawford, M. M. Kleb, V. S. Connors, R. J. Bendura, J. L. Raper, G. W. Sachse, J. C. Gille, L. Emmons, and C. L. Heald (2003), Transport and Chemical Evolution over the Pacific (TRACE-P) aircraft mission: Design, execution, and first results, *J. Geophys. Res.*, *108*(D20), 9000, doi:10.1029/2002JD003276.
- Leitch, W. R., et al. (2009), Evidence for Asian dust effects from aerosol plume measurements during INTEX-B 2006 near Whistler, BC, *Atmos. Chem. Phys.*, *9*, 3523–3546, doi:10.5194/acp-9-3523-2009.
- Li, Z., et al. (2007a), Aerosol optical properties and its radiative effects in northern China, *J. Geophys. Res.*, *112*, D22S01, doi:10.1029/2006JD007382.
- Li, Z., H. Chen, M. Cribb, R. Dickerson, B. Holben, C. Li, D. Lu, Y. Luo, H. Maring, and G. Shi (2007b), Preface to special section on East Asian Studies of Tropospheric Aerosols: An International Regional Experiment (EAST-AIRE), *J. Geophys. Res.*, *112*, D22S00, doi:10.1029/2007JD008853.
- Loeb, N. G., N. Manalo-Smith, S. Kato, W. F. Miller, S. K. Gupta, P. Minnis, and B. A. Wielicki (2003), Angular distribution models for top-of-atmosphere radiative flux estimation from CERES instrument on the TRMM satellite, Part I: Methodology, *J. Appl. Meteorol.*, *42*, 240–265, doi:10.1175/1520-0450(2003)042<0240:ADMFTO>2.0.CO;2.
- Martins, J., D. Tanré, L. Remer, Y. Kaufman, S. Mattoo, and R. Levy (2002), MODIS cloud screening for remote sensing of aerosols over oceans using spatial variability, *Geophys. Res. Lett.*, *29*(12), 8009, doi:10.1029/2001GL013252.
- Matthews, G., K. Priestley, P. Spence, D. Cooper, and D. Walikainen (2005), Compensation for spectral darkening of short wave optics occurring on the Cloud's and the Earth's Radiant Energy System, Earth Observing Systems X, *Proc. SPIE*, *5882*, 588212, doi:10.1117/12.618972.
- Murayama, T., et al. (2001), Ground-based network observation of Asian dust events of April 1998 in East Asia, *J. Geophys. Res.*, *106*(D16), 18,345–18,359, doi:10.1029/2000JD900554.

- Qiu, J. H., and J. Sun (1994), Optical remote sensing of the dust storm and the analysis, *Chin. J. Atmos. Sci.*, *18*, 1–10.
- Remer, L., et al. (2005), The MODIS aerosols algorithm, products, and validation, *J. Atmos. Sci.*, *62*, 947–973, doi:10.1175/JAS3385.1.
- Sun, J., M. Zhang, and T. Liu (2001), Spatial and temporal characteristics of dust storms in China and its surrounding regions, 1960–1999: Relations to source area and climate, *J. Geophys. Res.*, *106*(D10), 10,325–10,333, doi:10.1029/2000JD900665.
- Tanré, D., Y. Kaufman, M. Herman, and S. Matoo (1997), Remote sensing of aerosol properties over oceans using the MODIS/EOS spectral radiances, *J. Geophys. Res.*, *102*(D14), 16,971–16,988, doi:10.1029/96JD03437.
- Tanré, D., Y. J. Kaufman, B. N. Holben, B. Chatenet, A. Karnieli, F. Lavenu, L. Blarel, O. Dubovik, L. A. Remer, and A. Smirnov (2001), Climatology of dust aerosol size distribution and optical properties derived from remotely sensed data in the solar spectrum, *J. Geophys. Res.*, *106*(D16), 18,205–18,217, doi:10.1029/2000JD900663.
- Tsunematsu, N., K. Kenji, and T. Matsumoto (2005), The influence of synoptic-scale air flow and local circulation on the dust layer height in the north of the Taklimakan Desert, *Water Air Soil Pollut. Focus*, *5*, 175–193, doi:10.1007/s11267-005-0734-z.
- Wielicki, B. A., B. R. Barkstrom, E. F. Harrison, R. B. Lee III, G. L. Smith, and J. E. Cooper (1996), Clouds and the Earth's Radiant Energy System (CERES): An Earth Observing System experiment, *Bull. Am. Meteorol. Soc.*, *77*, 853–868, doi:10.1175/1520-0477(1996)077<0853:CATERE>2.0.CO;2.
- Xia, X., H. Chen, Z. Li, P. Wang, and J. Wang (2007), Significant reduction of surface solar irradiance induced by aerosols in a suburban region in northeastern China, *J. Geophys. Res.*, *112*, D22S02, doi:10.1029/2006JD007562.
- 
- M. Cribb and Z. Li, Department of Atmospheric and Oceanic Science, University of Maryland, College Park, MD 20742, USA.
- X. Dong, T. Logan, R. Obrecht, and B. Xi, Department of Atmospheric Sciences, University of North Dakota, 4149 University Dr., Stop 9006, Grand Forks, ND 58202-9006, USA. (timothy.logan@und.nodak.edu)